

OPTICAL AND MICROSTRUCTURAL PROPERTIES OF SOL-GEL SPIN COATED $MgAl_2O_4$ THIN FILMS

S. VALANARASU^a, V. DHANASEKARAN^b, M. KARUNAKARAN^c,
T. A. VIJAYAN^d, I. KULANDAISAMY^a, R. CHANDRAMOHAN^d,
K. K. LEE^{e*}, T. MAHALINGAM^e

^aDepartment of Physics, Arul Anandar College, Karumathur, Madurai – 625 514, India

^bGraphene Research Institute, Sejong University, Seoul 143 – 747, Republic of Korea.

^cDepartment of Physics, Sethupathi Government Arts College, Ramanathapuram – 623 502, India.

^dDepartment of Physics, Sree Sevugan Annamalai College, Devakottai – 630 303, India.

^eDepartment of Electrical and Computer Engineering, Ajou University, Suwon 443-749, Republic of Korea.

Magnesium aluminum oxide ($MgAl_2O_4$) thin films were prepared by sol-gel spin coating method. The as-prepared films were calcined at 500°C for 12, 18 and 24 hours. The calcinated films were exhibited with polycrystalline in nature cubic structure. (311), (400) and (440) diffracted lines were preferentially oriented in $MgAl_2O_4$ thin films. The crystallite size, lattice constant, microstrain, dislocation density, stacking fault probability and number of crystallites were calculated to study the indeed microstructural analysis of $MgAl_2O_4$. Tauc's plots were used to estimate the optical band gap energy and were observed in the range of 3.11-3.33 eV for 12-24 hours calcined $MgAl_2O_4$ thin films, respectively. The optical dispersion parameters were calculated using Spitzer-Fan model. Also, other refractive indices and complex dielectric constants were intensely discussed. The morphological studies were depicted the surface nature of the films. The electrical conductivity and activation energy values were discussed with calcinating time variations.

(Received April 5, 2015; Accepted June 10, 2015)

Keywords: Thin films; chemical synthesis; X-ray diffraction; Microstructure; Optical properties

1. Introduction

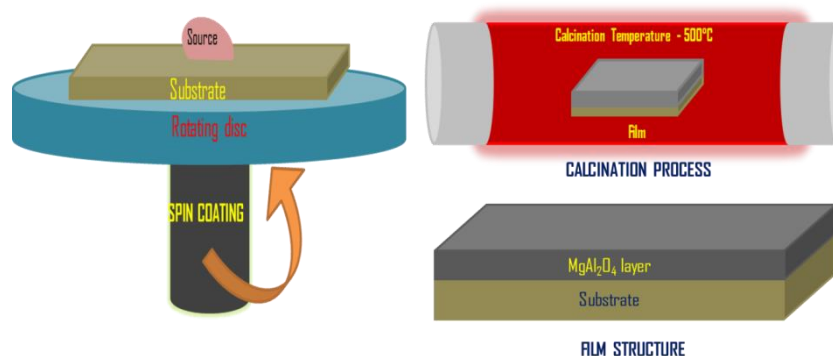
Magnesium aluminate ($MgAl_2O_4$) have attracted in recent researchers due to their high melting point, good chemical stability and mechanical strength, spinel-type solid. $MgAl_2O_4$ thin films have many applications in the various fields of materials science [1,2]. There is many reports available in the utilization of magnesium-aluminate spinel as catalysts or catalysts support in the fields of environmental catalysis, petroleum processing and fine chemicals production [3,4]. In addition, transparent $MgAl_2O_4$ have flexible physical properties in room temperature and higher temperature such as strong corrosion resistance, high resistance, excellent mechanical properties and optoelectronic properties [5, 6]. The $MgAl_2O_4$ based research have been under progress for many years for various applications in the basis of high temperature and millimeter wave communication systems [7, 8]. $MgAl_2O_4$ was also cited as an important base catalyst which have efficiently catalyzes the coupling reactions of short chain linear alcohols and mercaptan oxidation [9]. $MgAl_2O_4$ is synthesized by many physical and chemical techniques such as, conventional solid-state-reaction, sol-gel, MOCVD, aerosol method, polymeric precursor synthesis, spray

* Corresponding authors: keekeun@ajou.ac.kr

pyrolysis, pulsed laser deposition and organic gel-assisted citrate complexation, spark plasma sintering [10–18]. Among other methods, spin coating is a simple and low cost technique for thin film fabrication technology. In this work was done by sol-gel spin coating using precursor consisting of magnesium nitrate and aluminium nitrate. Sol-gel spin coating route prepared MgAl_2O_4 thin films was calcined at 500°C for 12, 18 and 24 hours. The lower time calcined film does not emit the precise nature of MgAl_2O_4 thin. The various time such as 12, 18 and 24 hours calcined MgAl_2O_4 thin films structural, surface morphological, compositional, electrical and optical absorption properties were studied using by X-ray diffraction (XRD), scanning electron microscopy (SEM), energy dispersive analysis by X-rays (EDAX) analysis, I-V studies and UV-vis spectroscopy, respectively.

2. Experimental details

MgAl_2O_4 thin films were prepared using low cost sol-gel spin coating route followed by calcination process and preparation scheme is presented in scheme 1. In this film preparation, we have used as a solution bath precursors of magnesium nitrate ($\text{Mg}(\text{NO}_3)_2 \cdot 6\text{H}_2\text{O}$), aluminium nitrate ($\text{Al}(\text{NO}_3)_3$), and ethanol ($\text{C}_2\text{H}_5\text{OH}$). A 0.1 M Mg ion solution is first prepared by $\text{Mg}(\text{NO}_3)_2$ thoroughly in $\text{C}_2\text{H}_5\text{OH}$. Also, 0.2 M aluminium nitrate is mixed as an Al source into that solution. Nitric acid was then added into the solutions which is act as a stabilizer. Sonication process was performed to the solution at 50°C for 20 minutes. Then the solutions are heat and stirred at 80°C for 3 hours and it followed by ageing process for 24 hours. In this work, cleaned glass was used as the substrate. To remove all residual on the glass, they were cleaned using acetone, methanol and deionized water in the ultrasonic bath in 10 minutes. MgAl_2O_4 thin films were then deposited on the substrate using spin coating method at the deposition parameter was set to 3000 rpm for 30 seconds. The prepared MgAl_2O_4 thin films were then dried at 200°C for 5 minutes. The deposition and drying process were repeated several times to achieve the desired film thickness. After the multi-coating process completion, calcinating of MgAl_2O_4 films was carried out at 500°C for 12, 18 and 24 hours. The prepared film films were characterized using following instruments. The deposited film thickness were measured using a stylus profilometer (Mitutoyo SJ-301) equipped with diamond needle. X-ray diffractograms were recorded using X'PERT PRO Panalytical diffractometer using Cu-K_α ($\lambda = 0.154 \text{ nm}$) as a source radiation. The energy dispersive analysis by X-ray spectrometer (EDS) attached FEI QUANTA scanning electron microscopy (SEM) analyses were performed for morphological and compositional studies. The optical properties were studied using UV-Vis-NIR spectrophotometer (PERKIN ELMER LAMDA 9).



Scheme 1 Schematic diagram of film preparation processes and film structure

3. Results and discussion

X-ray diffraction is an important tool to identify structural and microstructural properties of MgAl_2O_4 spinel structure films surface. X-ray diffraction patterns are recorded for various

times calcined MgAl_2O_4 thin films as shown in fig. 1. X-ray diffraction studies revealed that the deposited films are polycrystalline in nature with face centred cubic structure. X-ray diffraction pattern shows that the diffraction peaks at an angles 2θ 19.27° , 31.47° , 36.57° , 44.73° , 59.22° and 65.02° corresponding to crystallographic orientations (111), (220), (311), (400), (511) and (440), respectively. The observed peaks “d” spacing values are in good agreement with standard JCPDS card no. 89-1627 for MgAl_2O_4 film. The strongest diffraction peaks are appeared at (311) (400) and (440) plane which is a clear prediction of the mixed orientation. The peak sharpness and intensities are increased with increase of calcinating time. The observed diffraction pattern revealed the crystallinity of the film is increased with calcinating time. However, no other impurities related diffraction plane and novel peaks are not observed in these diffraction patterns. From the observed diffraction patterns, we have identified that the strong structural relation with calcinating time for MgAl_2O_4 films. We have further discussed about the microstructural properties of MgAl_2O_4 thin films for expose the obvious evidence the enhancement of microstructural enhancement.

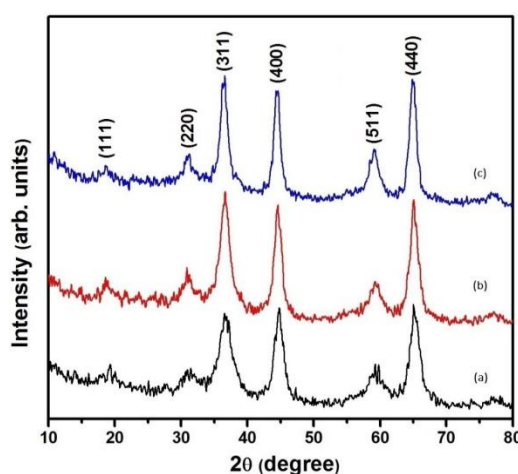


Fig. 1 X-ray diffraction patterns of various time calcined MgAl_2O_4 thin films (a) 12 (b) 18 and (c) 24 hours

The three diffraction lines are predominantly oriented X-ray diffraction patterns as shown in fig. 1. Hence, we have used the average values for the microstructural parameters evaluation for the exact estimation. From the (hkl) planes, the lattice constants are evaluated using the relation,

$$d = \frac{a}{\sqrt{h^2 + k^2 + l^2}} \quad (1)$$

where d is the inter-planar spacing of the atomic plane. From the X-ray diffraction line broadening, inter atomic distance between the two atoms are decreased with increase of calcinating time as shown in fig. 2. The observed d -spacing values are used to determine the lattice constant of MgAl_2O_4 thin films. The d -spacing value is directly proportional to the lattice constants values. The blue shift is observed in this lattice constant values also standard value is clearly indicated using straight line in fig. 2. The microstructural parameters are calculated using an X-ray diffraction patterns. The full-width at half maximum (FWHM) value is an important key parameter to determine microstructural properties of MgAl_2O_4 thin films. The variation of FWHM as a function of calcinating time is shown in fig.3. FWHM values are linearly decreased with increase of calcinating time which can be due to the increment of peak intensity and sharpness. Further we have analyzed the crystallite size variation with calcinating time shown in fig. 3. The crystallite size (D) is calculated using conventional Debye-Scherrer's formula. The crystallite size value of MgAl_2O_4 thin films are obtained from full width at half maximum which can be expressed as linear combination of contributes from the particle size, D . The origin of the crystallite size is related to the lattice misfit, which in turn depends upon the sample preparation. The crystallite size

can be controlled by adjusting calcinating time. The crystallite size is found to be in the range between 9 and 14 nm for calcinating time from 12 to 24 hours shown in fig. 3. The crystallite size is found to be increase gradually with increase calcinating time it may be due to decrement of FWHM values.

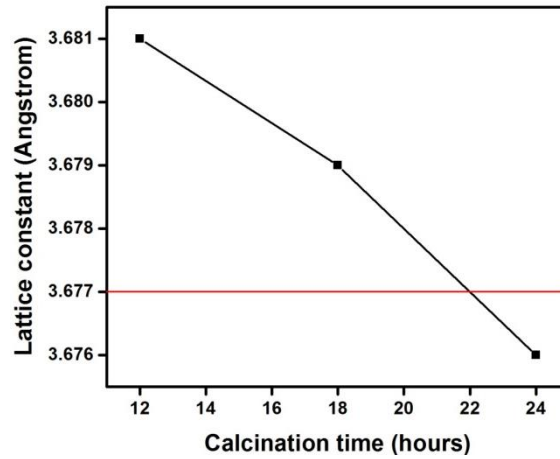


Fig. 2 Lattice constants variations of different time calcined $MgAl_2O_4$ thin films

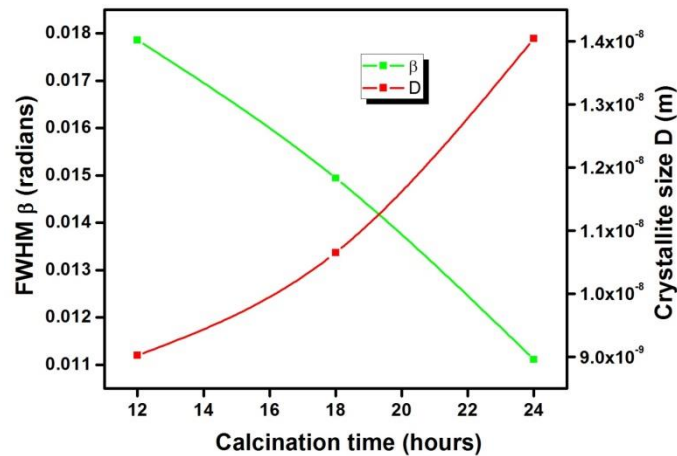


Fig. 3 Variations of FWHM and crystallite size as a function of calcination time for $MgAl_2O_4$ thin films

Fig. 4 is represented that the micro strain (ϵ) and stacking fault probability (α) variations in the key role of calcinating time. The micro strain ϵ is calculated using the relation [19],

$$\frac{\beta \cos \theta}{\lambda} = \frac{1}{D} + \epsilon \frac{\sin \theta}{\lambda} \quad (2)$$

where λ is wavelength and θ is Bragg's angle. The stacking fault probability was calculated by measuring the peak shift and tangent values of diffracting angle,

$$\alpha = \left(\frac{2\pi^2}{45\sqrt{3}} \right) \left(\frac{\Delta(2\theta)}{\tan \theta} \right) \quad (3)$$

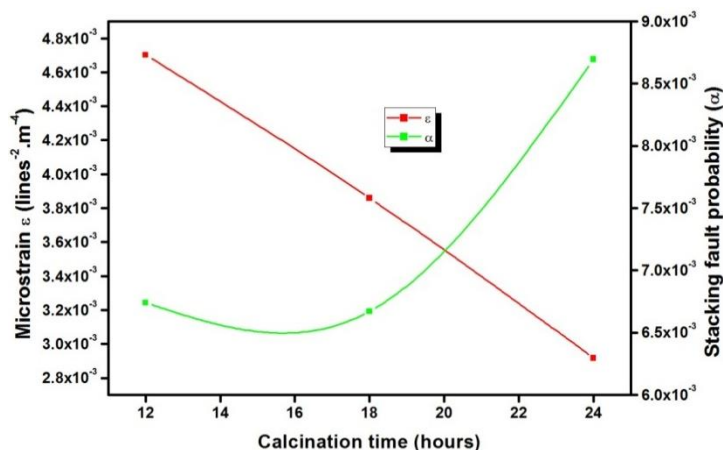


Fig. 4 Variations of micro strain and stacking fault probability as a function of calcination time for MgAl_2O_4 thin films

Generally the crystallite size is indirectly proportional to micro strain values. The linear decrement of micro strain values is observed from 4.7 to $2.9 \times 10^{-3} \text{ lines}^{-2}/\text{m}^{-4}$ for 12 to 24 hours calcined MgAl_2O_4 thin films. This observation is clearly represented the enhancement of crystallite size in MgAl_2O_4 thin films. The stacking fault probability value is observed at 6.7×10^{-3} for 12 hours calcined MgAl_2O_4 thin film. This value is slightly increased to 6.6×10^{-3} for 18 hours calcined thin film. This type of variation can be due to the variations of standard and observed diffraction angles. The rapid increment is observed at 8.6×10^{-3} in stacking fault probability shown in fig. 4 for 24 hours calcined thin film due to lower diffraction angle variations. These variations are suggested that the crystallinity and preferential orientation increases with calcinating time.

The dislocation density (δ) defined as the length of dislocation lines per unit volume of the crystal, is evaluated from the crystallite size D and microstrain (ϵ) by the relation,

$$\delta = \frac{15\epsilon}{aD} \quad (4)$$

where 'a' is lattice constant. The number of crystallites per unit area (N) of the films is determined with the using formula,

$$N = \frac{t}{D^3} \quad (5)$$

where t is thickness of the film, N is number of crystallites per unit area and D is crystallite size. Fig. 5 shows dislocation density (δ) and number of crystallites per unit area (N) of variations as function of calcinating time for MgAl_2O_4 thin films. The dislocation density and number of crystallites per unit area are decreasing with increase of calcinating time. The minimum value of dislocation density and number of crystallites per unit area are found to be $8.9 \times 10^{14} \text{ lines}/\text{m}^2$ and 3.6×10^{16} , respectively, for the film calcined at 24 hours. These spectral variations such as rapid decrement of dislocation density and number of crystallites values with calcinating time can be attributed to the enhancement of crystallite size.

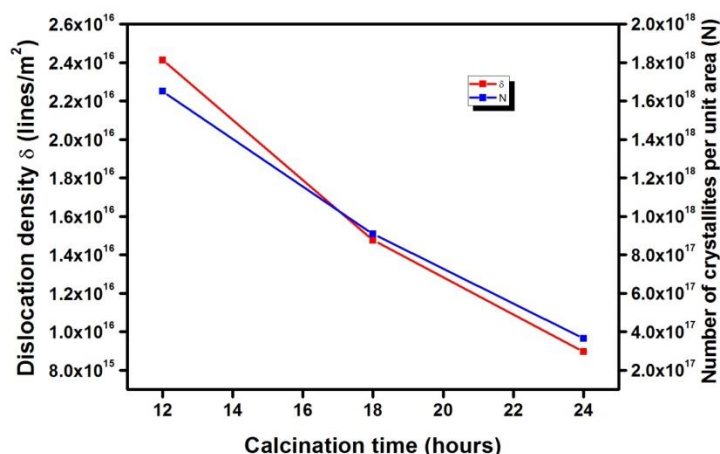


Fig. 5 Variations of dislocation density and number of crystallites per unit area as a function of calcination time for $MgAl_2O_4$ thin films

The film thickness is decreased with increase of calcinating time as given in table 1. The increase of crystallite size with decrease of film thickness is confined the quantum confinement. Thin films of $MgAl_2O_4$ thin thickness are estimated to be 460-320 nm and also their observed optical transmission properties aspect like a monotonous. The optical properties of metal oxide thin films are studied using transmission values. Some interesting properties may be explored by metal oxide thin films. In this case, absorption and transmission experiments may take very important information enabling observation and evaluation of material constants of metals and pick out thin effects in metal oxide films [23]. The highly affordable properties are observed in thin metal oxide films with a critical thickness – thickness of transition between continuous and island films.

Table 1 Film thickness, optical and electrical parameters of $MgAl_2O_4$ thin films

Calcination time (Hours)	Film thickness (nm)	Dispersion parameters				Optical conductivity $10^{14} s^{-1}$	Electrical conductivity $10^{-4} \Omega^{-1} \cdot cm^{-1}$	Activation energy eV
		E_0 (eV)	E_d 10^{-3} (eV)	M_{11} (10^{-3} eV)	M_{33} (10^{-2} eV) ²			
12	460	3.8 4	6.41	1.67	2.47	1.02	2.53	0.21
18	360	4.0 2	6.02	1.51	2.45	0.51	9.65	0.36
24	320	8.0 6	0.52	0.73	0.48	0.49	62.9	0.42

The prepared films have a maximum transmission percentage in the visible range. The absorption edge is observed at ~360 nm for 12, 18 and 24 hours calcined $MgAl_2O_4$ thin films it may be due to absorption of the glass substrate. The transmittance has increased with the wavelength as well as calcinating time and it is illustrated in fig. 6. The maximum value of transmission is exhibited at a constant place in the spectra, it is not dependent on the film thickness and it has obeyed the size of the crystallites. The transmittance spectra are observed the surface plasmons resonance indicating the crystallite sizes in the nanometre range. Mie theory and Maxwell-Garnet theory explained the surface plasmon resonance (SPR) in terms of higher moment oscillation and particle size [21, 22]. Although, it has been found that the width and peak position of the SPR are depends on the particle size, shape and environment [22]. The enhancement of

transmittance values can affect optical band gap values it may be due to the carrier concentration variations of the films. Also it can be due to the enhancement in the grain boundaries which is achieved during calcinating.

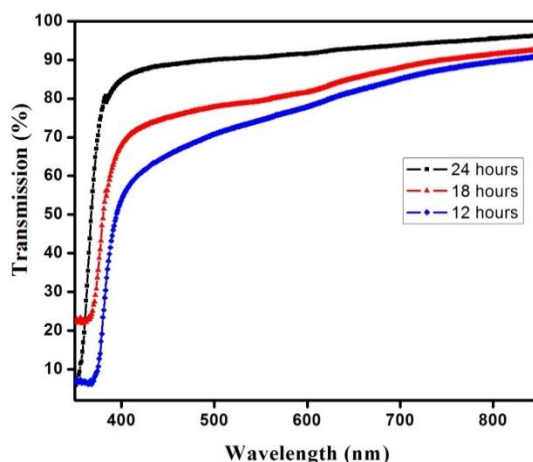


Fig. 6 Optical transmission variations as function of wavelength for different time calcined $MgAl_2O_4$ thin films

The nature of transition is determined using the following equation [23]. The band gap energy of the grown thin films can be determined by extrapolation of the linear part of the plot of $\alpha h\nu^2$ versus the incident radiation energy ($h\nu$), as shown in fig. 7; which indicates that the near band edge optical absorption coefficient has spectral dependence of only the joint density of states. The energy band gap of films is found to be in the range of 3.11–3.33 eV using the conventional Tauc's plot method (table 1). The band gap energy increases with increase of film thickness as well as crystallite size may be due to quantum confinement. It is attributed the blue shift of the optical absorption edge to the increasing crystalline quality of the $MgAl_2O_4$ thin films. However, the band gap can be changed by the alterations in the oxygen sites. The increase in the band gap may be associated with decrease in oxygen content in the film that might have been caused due to the more time of calcinating. The estimated values of optical transmittance of $MgAl_2O_4$ thin film is used to calculate the refractive index and the extinction coefficient. The refractive index was calculated using the Swanepoel's method [24]. Generally, the refractive index decreases as increase of calcinating time of $MgAl_2O_4$ thin films. The refractive index and extinction coefficient of the films decreased with increase of calcinating time is shown in fig. 8. The n and k of the films decreased linearly with the increase of calcinating time. It is evaluated that in the refractive index spectra, the lower thickness films exhibit a higher energy region, while the higher thickness films exhibit a lower energy region.

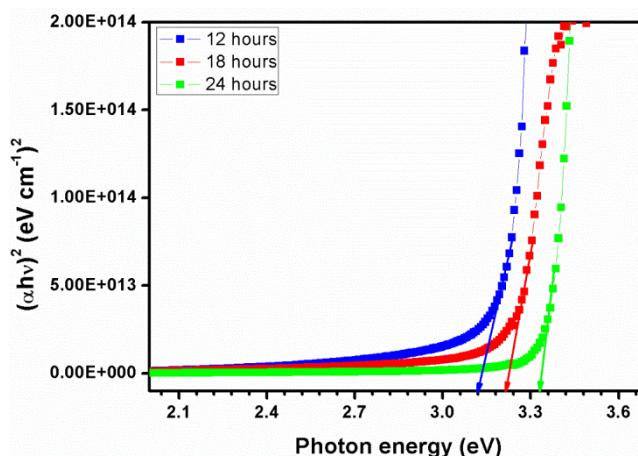


Fig. 7 Variations of Tauc's plot for various time calcined $MgAl_2O_4$ thin films

The real and imaginary parts of the dielectric constant were determined using the relation [25]. The prepared $MgAl_2O_4$ thin films optical properties are correlated with the frequency of incident light. The essential intrinsic substantial stuff is exhibited from dielectric constant value. The real part of dielectric constant is associated with the property of slowing down the speed of light in the material. The real part dielectric constant values are decreased as increase of calcinating time which may due to the decrement of refractive index values as shown in fig. 9. The imaginary part of dielectric constant values are decreased with calcinating time as well as wavelength, it could be obviously related to the extinction coefficient values. The dielectric suppression observed in this work could be also due to the atomic coordination-number imperfection, which dictates the size dependence of the crystal binding and the electron-phonon coupling, thus determines the entire band structure such as band gap expansion. The reduction in dielectric constant has been attributed to band gap should be lower the polarizability or the breaking of polarizable bonds at the surface.

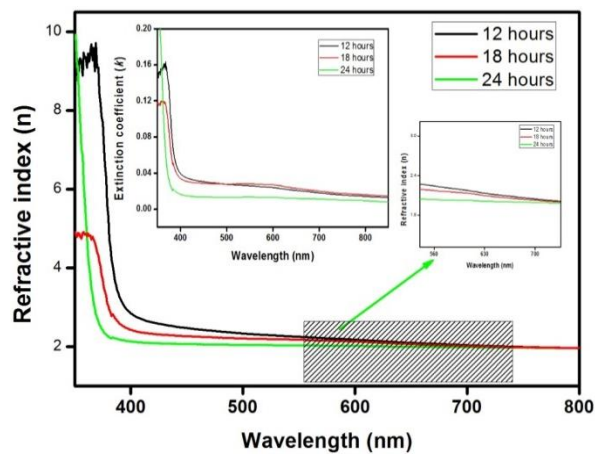


Fig. 8 Refractive indices variations for different time calcined $MgAl_2O_4$ thin films

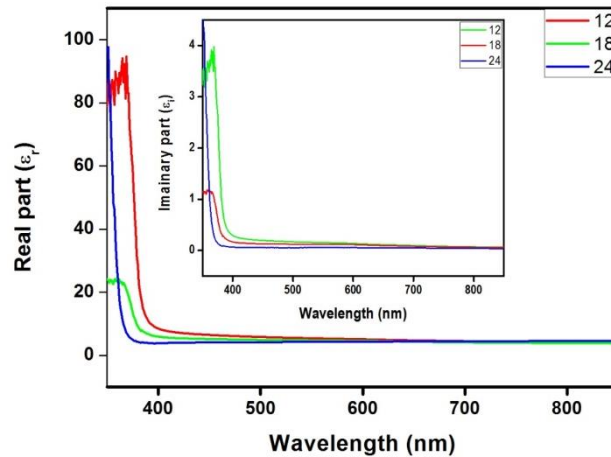


Fig. 9 Complex dielectric constants variations for different time calcined $MgAl_2O_4$ thin films

The optical conductivity values variations of various times calcined $MgAl_2O_4$ thin films are presented in table 1. The optical conductivity is determined using the usual relation

$$\sigma = \alpha n c \quad (6)$$

The optical conductivity of the films is estimated using equation (8). In this case MgO thin films optical conductivity decrease with the increase in calcinating time. This is may be due to the increase of band gap that increases with calcinating time. The spectral dependence of the refractive

index of many semiconductors can be evaluated by using the model proposed by Spitzer and Fan [26].

$$n^2 = 1 + \left[\frac{E_0 E_d}{E_0^2 - (h\nu)^2} \right] \quad (7)$$

To find out the dispersive parameters such as average excitation energy (E_0) and dispersion energy (E_d), we have followed the procedure [25]. Experimental verification of equation (7) can be obtained by plotting $(n^2 - 1)^{-1}$ versus $(h\nu)^2$ for MgAl_2O_4 thin films, which yields a straight line for normal behavior having the slope $(E_0 \times E_d)^{-1}$ and the intercept with the vertical axis equal to (E_0/E_d) . An affirmative linear curvature aberration from the longer wavelength is frequently observed owing to the negative contribution of lattice vibrations on the refractive index [27]. The values of the parameters E_0 and E_d can be estimated. Also optical spectra moments M_1 and M_3 are estimated using excitation energy (E_0) and dispersion energy. The estimated values are given in table 1.

Preliminary electrical conductivity studies carried out with two probe measurements on MgAl_2O_4 thin films indicated an improvement in electrical conductivity. The low temperature electrical resistance measurement is carried out in the temperature range 0-150°C using the two-point probe method. A constant low voltage (V) applied across the two electrodes and the current through the film was measured as a function of temperature. Fig. 10 shows that electrical conductivity against temperature of MgAl_2O_4 thin film calcined at three different time such as 12, 18 and 24 hours. The conductivity increases with increase of temperatures indicating the semiconducting nature of the MgAl_2O_4 films. The high value of conductivity may be attributed to the higher size of crystallites exhibited in the film. In general, in semiconductors, the passage mechanism is greatly influenced by the intercrystalline grain boundaries and strain fields associated with dislocation network [28]. This behavior may be explained from the temperature dependent electrical conductivity of the film surface. There is electron across the energy transition from the filled valence-band level to the unfilled conduction-band states. Therefore the thickness could affect the electrical conductivity in the lower temperature.

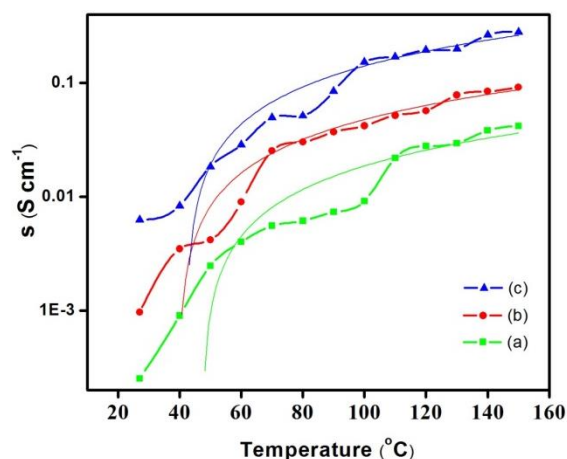


Fig. 10 Electrical conductivity variations for different time calcined MgAl_2O_4 thin films

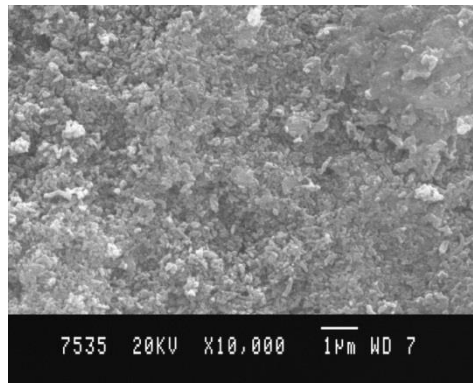


Fig. 11(a) SEM micrograph of 500°C calcined MgAl₂O₄ thin film at 12 hours

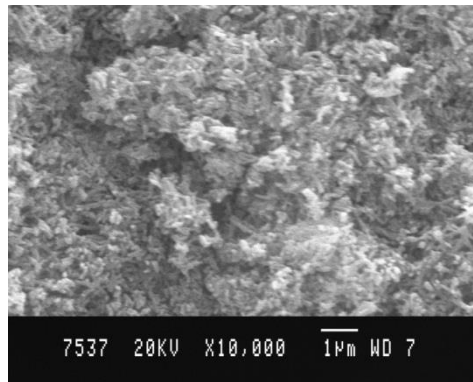


Fig. 11(b) SEM micrograph of 500°C calcined MgAl₂O₄ thin film at 18 hours

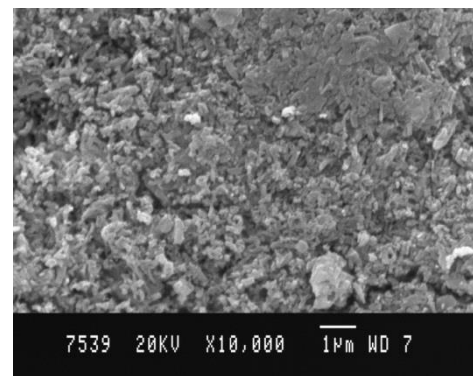


Fig. 11(c) SEM micrograph of 500°C calcined MgAl₂O₄ thin film at 24 hours

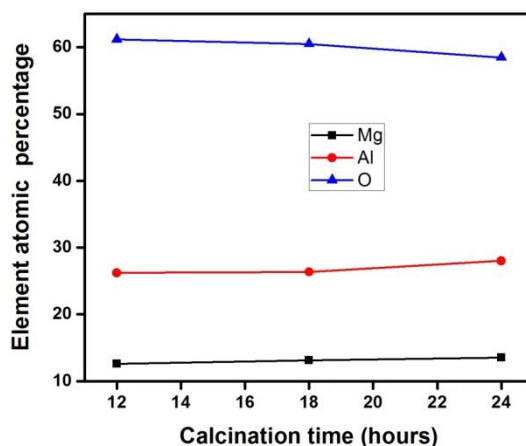


Fig. 12 Compositional variations for different time calcined MgAl_2O_4 thin films

The surface morphology of 12, 18 and 24 hours calcined MgAl_2O_4 thin films were examined by scanning electron microscopy (SEM). Fig. 11 (a-c) shows the SEM picture of MgAl_2O_4 for 12, 18 and 24 hours, respectively. The surface morphology of 12 hours calcined MgAl_2O_4 thin film reveals a number of compact bright contrast spots in nanoscale that could have been due to the stacked rods of polygonal cross section as shown in Fig. 11a. The 18 hours calcined MgAl_2O_4 thin morphology reveals that the surface of the film appear to be formed due to grains, and voids and coarse structure with little smaller cross section in fig. 11b. The lower time calcined films look very thin having a lot of irregularities and exhibiting inhomogeneous nature. The grain size is increased with calcinating time as shown in fig. 11(b) for 12 hours calcined MgO thin film surface. The spherically shaped grains are uniformly distributed to the surface of the films and also some voids are exhibited in few places of SEM picture. Fig. 11(c) represent the evenly distributed grains over the surface of the film. The sizes of the grains are found to be in the range between 200 and 250 nm. This result implies that there is an increase in nucleation over-growth and the deposits are more compact with uniform grain structure. An increase in the size of the crystallites with calcinating time is also evident from the SEM picture. However, 24 hours calcined films there is an increase in grain size and homogeneity. An increase in the size of the crystallites with calcination time is also evident from the SEM picture. No apparent changes of the surface morphologies are visible when the films are calcined in higher time. This may be due to the uniform thermal treatment gained by the sample during growth. Fig. 12 shows compositional variations of 12, 18 and 24 hours calcined MgAl_2O_4 thin films obtained using EDX analysis. The oxygen content has decreased with increase of calcinating time in the thin films in fig. 12. This oxygen content variation should be due to the absorption of oxygen during the calcinating. Also Mg and Al contents are slightly increased due to the calcinating time. This result is also consistent with X-ray diffraction analysis of the sample with cubic phase corresponding to MgAl_2O_4 thin formation.

4. Conclusions

The objective of the work was optical and micro structural studies on the various time calcined MgAl_2O_4 thin films grown over glass substrates by a low cost chemical bath deposition. The detailed discussion were incorporated in the calcinating time influence on the physical parameters of chemically grown MgAl_2O_4 structures. X-ray diffraction patterns revealed the polycrystalline cubic structure. The lower crystallite size was observed for 12 hours calcined film compared with 18 and 24 hours calcined films. It had been observed that the direct band gap energy increased from 3.11 to 3.33 eV for MgAl_2O_4 thin film calcined at 12 to 24 hours, respectively. We have proposed that the band gap energy variation may be due to the low oxygen content of the sample surface after thermal treatment. The refractive index and extinction

coefficient were showed some variation with calcinating time. The composition analysis was performed by EDX analysis and compositional variations have plotted against calcinating time. The electrical conductivity was increased with increase of temperature for various time calcined MgAl_2O_4 thin films. An increase in the size of the grains with calcination time was also evident from the SEM picture. The closest packed and crack-free structure was obtained for films calcined at maximum time. From the obvious discussion, MgAl_2O_4 based polycrystalline films are to be used in optoelectronic devices and gas sensors.

References

- [1] G. Mattoigno, G. Righini, G. Montesperelli, E. Traversa, *J. Mater. Res.* **9**, 1426 (1994).
- [2] A. Kuramata, K. Horino, K. Domen, K. Shinohara, T. Tanahashi *Appl. Phys. Lett.* **67**, 2521 (1995).
- [3] F. Pepe, M. Occhiuzzi, *J. Chem. Soc. Faraday Trans.* **90**, 905 (1994).
- [4] N. Guilhaume, M. Primet, *J. Chem. Soc. Faraday Trans.* **90**, 1541 (1994).
- [5] D.C. Harris, SPIE-the International Society for Optical Engineering, P.O. Box 10, Bellingham, WA, USA (1999).
- [6] S.M. Hosseini, *Phys. Status Solidi B* **245**, 2800 (2008).
- [7] G. Gilde, P. Patel, P. Patterson, D. Blodgett, D. Duncan, D. Hahn, *J. Am. Ceram. Soc.* **88**, 2747 (2005).
- [8] K.P. Surendran, P.V. Bijumon, P. Mohanan, M.T. Sebastian *Appl. Phys. A* **81**, 823 (2005).
- [9] J. Salmones, J.A. Galicia, J.A. Wang, M.A. Valenzuela, G. J. Mater. Sci. Lett. **19**, 1033 (2000).
- [10] J-H. Boo, S-B. Lee, S-J. Ku, W. Koh, C. Kim, K-S. Yu, Y. Kim, *Appl. Surf. Sci.* **169-170**, 581 (2001).
- [11] T. Misu, N. Sakamoto, K. Shinozaki, N. Adachi, H. Suzuki, N. Wakiya, *Sci. Technol. Adv. Mater.* **12**, 034408 (2011).
- [12] H. Jiang, Z. Cao, R. Yang, L. Yuan, H. Xiao, J. Dong, *Thin Solid Films* **539**, 81 (2013).
- [13] P. Fu, W. Lu, W. Lei, Y. Xu, X. Wang, J. Wu, *Ceram. Int.* **39**, 2481 (2013).
- [14] J.T. Bailey, R. Russell, *Am. Ceram. Soc. Bull.* **47**, 1025 (1968).
- [15] F. Federici Canova, A.S. Foster, M.K. Rasmussen, K. Meinander, F. Besenbacher, J.V. Lauritsen, *Nanotechnology* **23**, 325703 (2012).
- [16] E. Kostic, L. Momcilovic, *Ceramurgia International* **3**, 57 (1977).
- [17] H.C. Park, Y.B. Lee, K.D. Oh, F.L. Riley, *J. Mater. Sci. Lett.* **16**, 1841 (1997).
- [18] R. Sarkar, S.K. Das, G. Banerjee, *Ceram. Int.* **25**, 485 (1999).
- [19] V. Dhanasekaran, T. Mahalingam, *J. Alloys Compd.* **539**, 50 (2012).
- [20] A. Axelevitch, B. Gorenstein, G. Golan, *Physics Procedia* **32**, 1 (2012).
- [21] G. Mie, *Ann. Phys.* **25**, 377 (1908).
- [22] Ahmadi TS, Logunov SL, El-Sayed MA. (1996) Picosecond dynamics of colloidal gold nanoparticles, *J. Phys. Chem.* 100:8053-8056.
- [23] V.F. Kamalov, R. Little, S.L. Logunov, M.A. El-Sayed, *J. Phys. Chem.* **100**, 6381 (1996).
- [24] Swanepoel R. (1983) Determination of the thickness and optical constants of amorphous silicon *J. Phys. E* 16:1214-1222.
- [25] V. Dhanasekaran, T. Mahalingam, R. Chandramohan, J-K. Rhee, J.P.Chu, *Thin Solid Films* **520**, 6608 (2012).
- [26] W.G. Spitzer, H.Y.Fan, *Phys. Rev.* **106**, 882 (1957).
- [27] S.A. Maier *Plasmonics: Fundamentals and Applications*, Springer, USA (2007).
- [28] S. Valanarasu, V. Dhanasekaran, M. Karunakaran, T.A Vijayan, R. Chandramohan, T. Mahalingam, *Microstructural, J. Mater. Sci.: Mater. Electron.* **25**, 3846 (2014).